



Radiomic analysis of the optic nerve at the first episode of acute optic neuritis: an indicator of optic nerve pathology and a predictor of visual recovery?

Michaela Cellina¹ · Marta Pirovano² · Matteo Ciocca² · Daniele Gibelli³ · Chiara Floridi⁴ · Giancarlo Oliva¹

Received: 25 February 2020 / Accepted: 25 November 2020 / Published online: 3 January 2021
© Italian Society of Medical Radiology 2021

Abstract

Objective Retinal nerve fiber layer thickness (RNFL) is a biomarker of neuroaxonal loss and index of visual function in multiple sclerosis (MS). We aimed to assess the correlation between radiomic features and RNFL, visual acuity (VA) at patients' presentation, visual outcome (VO), and clinical diagnosis.

Methods We reviewed imaging and clinical data of 25 patients with a first episode of optic neuritis (ON) (14 females, 11 males; 5 bilateral ON; 7 left ON; 13 right ON). All patients underwent a complete ophthalmological assessment, including visual acuity and RNFL, neurological evaluation, orbits MRI. Segmentation of the optic nerves was performed through 3D slicer open software to get radiomics analysis. All patients underwent a complete neuro-ophthalmological follow-up at 6 months to assess the VO, classified as: complete recovery, partial recovery, deficit persistence/relapse, or visual worsening and were diagnosed as MS or clinically isolated syndrome.

Results We observed significant correlations between radiomic features and RNFL and between radiomic features and VA. Regression model analysis identified 1 radiomic feature with significant association with VO (Gray Level non-uniformity Normalized, $p=0.004$) and 6 radiomic features with significant correlation with diagnosis (High Gray Level Zone Emphasis, $p < 0.001$; Entropy, $p < 0.001$, for T1 segmentation; Mean Absolute Deviation, $p < 0.001$; Coarseness < 0.001 ; Small Area Low Gray Level Emphasis, $p < 0.001$; Contrast, $p = 0.008$, for STIR segmentation).

Conclusion Orbits MRI analysis at the first episode of ON has the potential to assess the visual function and VO in ON patients, and predict MS development.

Keyword Radiomics · Optic neuritis · Optic nerve · Orbit magnetic resonance · RNFL

Background

Optic neuritis (ON) is an acute inflammatory demyelinating disorder, that can be isolated or associated with other neurological diseases like neuromyelitis optica or multiple sclerosis (MS) [1–4].

The three most common symptoms are unilateral, subacute visual loss, periocular pain in eye movements, dyschromatopsia, without systemic or other neurological symptoms [3, 5].

Optical coherence tomography (OCT) is a non-invasive and highly reproducible imaging technique commonly used in ophthalmology to visualize and quantify the retinal layers and is considered an essential tool in neuro-ophthalmologic practice. It allows direct visualization of the optic nerve head, imaging unmyelinated central nervous system (CNS) axons within the retina, the retinal nerve fiber layer (RNFL),

✉ Michaela Cellina
michaela.cellina@asst-fbf-sacco.it

¹ Radiology Department, ASST Fatebenefratelli Sacco, Piazza Principessa Clotilde 3, 20123 Milan, Italy

² Neurology Department, ASST Fatebenefratelli Sacco, Piazza Principessa Clotilde 3, 20123 Milan, Italy

³ Dipartimento Di Scienze Biomediche Per La Salute, Università Degli Studi Di Milano, Via Mangiagalli 31, 20121 Milan, Italy

⁴ Department of Radiology - Division of Special and Pediatric Radiology, University Hospital "Umberto I - Lancisi - Salesi", Via Conca 71, 60126 Ancona, AN, Italy

providing a measure of its thickness and information about optic nerve head topography and macular volume. The RNFL thickness is used as a marker of axonal and neuronal loss in neurological diseases involving the anterior visual pathways, as MS [3, 6].

Visual recovery after ON is variable and difficult to predict [7]: data regarding the ability of baseline orbits magnetic resonance imaging (MRI) to predict visual outcome (VO) are discordant [8–12].

ON is a common manifestation of MS and precursor to its development. The presence of inflammatory demyelination and axonal loss in ON parallels the abnormalities observed in other white matter structures. Evidence from research in ON can be applied to the larger group of patients affected by MS [13]: therefore, the optic nerve represents a readily accessible target to establish the efficacy of MS treatments that aim at restoring neurological function.

Radiomics is an emerging field in quantitative imaging, consisting of the extraction of advanced imaging features from conventional modalities [13–15]. Radiomic features provide diagnostic, predictive, and prognostic information, especially in the oncologic field: in fact, they not only represent an objective and quantitative way to assess tumor phenotype but also showed a promising role in the prediction of treatment response, providing valuable information for tailored therapy [16]. The usefulness of texture analysis, a type of radiomic analysis for tissue heterogeneity assessment, has been investigated in predicting VO after ON in only one group of patients with relapsing–remitting MS or clinically isolated syndrome (CIS), on a 3 T magnet [17].

To our knowledge, no case series about patients with the first episode of ON, or regarding radiomic analysis of ON have been reported yet.

Therefore, our aims were: (1) to explore the role of radiomics in ON patients without a history of demyelinating disorders, analyzing the correlation between radiomic features and RNFL thickness at OCT and between radiomic features and visual acuity (VA) at baseline, and (2) to assess if radiomic data can predict VO and MS development.

Methods

This retrospective study has been approved by our Institutional Review Board, and written informed consent was provided by patients.

Patients

We reviewed the ophthalmological, neurological, and imaging data of patients who presented to our emergency department (ED) with the first episode of ON from January 2015 to January 2017 ($N=85$).

Exclusion criteria were as follows: previous episodes of ON; a history of demyelinating disorders, of known ophthalmological diseases and known immunological/infective disorders; the lack of complete ophthalmological, neurological, imaging data; the time between symptoms onset and presentation > 14 days; timing between ED arrival and MRI > 14 days; lack of follow-up.

We, therefore, included 25 patients, 14 females and 11 males (age range: 21–43 years; mean age: 30.7 years). 13 patients had right ON, 7 had left eye ON, and 5 had bilateral ON, for a total of 30 affected eyes.

The time between symptoms onset and ED arrival was 1–7 days (mean: 3 ± 4 days).

Ophthalmological and laboratory tests

At the arrival, every patient underwent a complete ophthalmological examination, including fundoscopy, VA assessment, visual field, OCT and visual evoked potential (VEP), and a neurological evaluation.

VA was measured according to Snellen chart (decimal) and was divided into 3 groups: severe deficit (mm-4/10), intermediate deficit (5–7/10), slight deficit (8/10, 9/10). Light perception and *motus manus* (mm) were assigned a value of 0.

The visual field was investigated with Humphrey perimetry using the SITA algorithm (Zeiss Meditech, version 1.2.40.43).

VEPs were performed on a Natus System (software version Nicolet EDX 21.1; Natus Neurology, Pleasanton, CA), with patients at 1 m from the computer screen and asked to maintain visual fixation on a red cross in the center of an alternating checkerboard pattern of black and white squares (check size 32') at 100% contrast. Abnormal VEPs findings included increased latencies, reduced amplitudes, and abnormal waveforms (Table 1).

Every OCT was acquired on the same machine (Spectralis version 6.3.2, Heidelberg Engineering™), after inducing mydriasis with 1% tropicamide. The software automatically provided the results on a color-coded graphic display, showing the RNFL thickness in μm in the retinal quadrants [temporal (T), temporal superior (TS), temporal inferior (TI), nasal (N), nasal superior (NS), nasal inferior (NI)], and an average global value (G) (Fig. 1).

Patients' ophthalmological features are listed in Table 1

To exclude metabolic, infective, and autoimmune ON causes, a series of blood tests were performed, as well as tests for Aquaporin 4-IgG and myelin oligodendrocyte glycoprotein-IgG; these examinations were negative [18]. Cerebrospinal fluid for oligoclonal bands detection was collected.

After the execution of the ophthalmological examinations, intravenous steroid treatment was started.

Table 1 This table list patients' characteristics regarding their demographics, the ophthalmological symptomatology at their arrival in our emergency department, the results of the ophthalmological tests at their arrival: visual field (VF), visual acuity according to Snellen chart, optic disk appearance at funduscopy, average RNFL thickness on OCT, the findings at visual evoked potentials (VEP). When the total is indicated as 25, it refers to the number of patients, when it is indicated as 30, it refers to the number of affected eyes

Patients' ophthalmologic characteristics	n/total
Right ON	13/25
Left ON	7/25
Bilateral ON	5/25
Pain on eye movement	24/25
Dyschromatopsia	11/25
Normal VF	3/30
VF central scotoma	12/30
VF sectorial deficit	7/30
> 2 sectorial deficits	2/30
VF subtotal / total scotoma	6/30
Visual acuity range	mm-9/10
Mean visual acuity	3.5/10 ± 2.7/10
Normal appearance at funduscopy	10/30
Optic disk swelling at funduscopy	15/30
Blurred margins of the optic disk	5/30
Pale optic disk	0/30
Exudates/hemorrhages at funduscopy	0/30
Global average RNFL within normal range	10/30
Global average RNFL increased	17/30
Global average RNFL reduced	1/30
Global average RNFL borderline	2/30
Increased latencies at VEP	30/30
Reduced amplitude at VEP	6/30
Abnormal waveform at VEP	15/30

mm = moto manus

MRI

All patients underwent brain, orbits, cervical spine MRI on a 1.5 T scanner, (Avanto, Siemens) with an 8-channel head coil, and gadolinium injection (1 ml/10 kg of gadobutrol, Gadovist, Bayer Schering Pharma). Our protocol included an orbital SPACE Short Time Inversion Recovery (STIR) acquisition (FOV, 200 × 198 mm; matrix, 218 × 256; voxel, 0.9 × 0.9 × 0.9 mm; TR, 3800 ms; TE, 213 ms, inversion time, 160 ms) and an axial post-contrast T1 Fat Saturated Spin Echo (FOV, 190 × 190 mm; matrix, 160 × 320; voxel, 1.2 × 0.6 × 3.0 mm; TR, 550 ms; TE, 17 ms; flip angle, 90°), 5 min post gadolinium administration. The time between patients' arrival and MRI execution was 1–7 days (mean time: 3 ± 4 days).

Radiomics analysis

We extracted radiomic features from both STIR and T1 acquisitions through a manual segmentation of the whole affected optic nerve, from the intraorbital portion to optic chiasm, by the same operator on an open-source platform, 3D slicer, version 4.9 (Harvard University) [19, 20] (Fig. 2), that automatically calculated radiomic parameters corresponding to the selected area.

104 radiomic features belonging to 7 families (Gray Level Dependence Matrix, Gray Level Co-occurrence Matrix, First Order Statistics, Shape-based, Gray Level run length Matrix, Gray Level Size Zone Matrix, Neighboring Gray tone Difference Matrix) were extracted from each raw image, without applying any image filter. Since optic nerves were the subject of our analysis, we did not include any shape features, and, therefore, we considered a total of 91 radiomic features.

The same segmentation procedure was performed for T1 sequences on a control group of 25 patients, selected from our MRI database, with similar demographics, who underwent MRI for benign disorders (lacrimal gland epidermoid cysts and orbital vascular lesions).

Follow-up

Each patient underwent a clinical follow-up of at least 12 months (mean follow-up time: 16 ± 4 months). Ophthalmological evaluation including VA was performed at 6 months to establish the VO, with timing following previous studies describing dominant visual recovery within this period [17, 21].

VO was classified as (1) complete recovery: VA back to the value before ON, (2) partial recovery: recovery ≥ 50% compared to the value before ON, (3) stable deficit: recovery < 50%, or visual deficit persistence, (4) visual worsening.

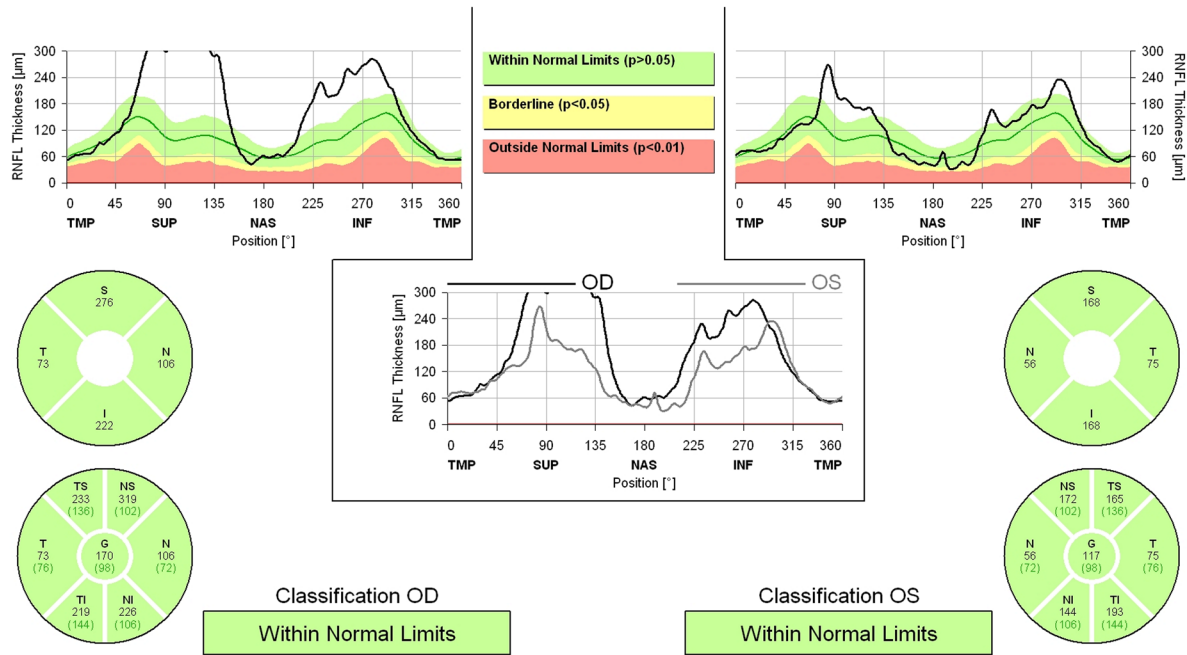
9/30 eyes had complete VA recovery, 13/30 had partial recovery, 8/30 manifested a deficit persistence, 0/30 eyes had visual worsening. Mean VA at follow-up was 7 ± 1/10.

11/25 patients received a diagnosis of MS, 14/25 received a diagnosis of CIS, based on revised McDonald criteria [22].

Statistical analysis

Statistical analysis was performed using SPSS, version 20.0. Pearson's correlation coefficient was calculated to determine the correlations between radiomic features extracted from T1 sequences and RNFL thickness for the retinal quadrants, we then included radiomics variables with a p value < 0.05 gender, and sex and age as nuisance covariates, in the building of a multivariate logistic regression model using RNFL thickness as dependent variables.

Radiomic features were used in a least absolute shrinkage selection operator (LASSO) regression model to reduce



Software Version: 6.3.2

www.HeidelbergEngineering.com

RNFL Single Exam Report OU

Fig. 1 Example of an OCT examination. For both the right and left eye, a graphical representation of RNFL thickness is provided. The values of RNFL thickness are available for all retinal quadrants: TI: temporal inferior; T: temporal; TS: temporal superior; NS: nasal

superior; N: nasal; NI: nasal inferior. In the center of the circle, G value represents the global average RNFL thickness. In brackets, the reference values of RNFL thickness in accordance with the subject’s age are indicated

the number of features in the training cohort to identify the features most relevant to VA, outcome, and diagnosis.

Bonferroni’s correction was applied taking into consideration the number of groups in comparison ($p < 0.01$).

Statistically significant differences between patients and control groups were assessed through Student’s t-test ($p < 0.05$), after we checked the variables for normality with a one-sample Kolmogorov–Smirnov test.

Results

At multivariate logistic regression, we observed significant correlations between RNFL thickness and radiomic features extracted from T1 sequences mainly belonging to the First Order Features (Skewness, Median, 90° Percentile) and Gray Level Size Zone Matrix (Gray Level Non-Uniformity, Zone Entropy, High Gray Level Zone Emphasis) (Table 2).

Regression model analysis highlighted formulae between radiomic parameters and VA (R^2 : 0.44 for T1 segmentation; R^2 : 0.78 for STIR segmentation), outcome (R^2 : 0.36 for T1 segmentation; R^2 : 0.88 for STIR segmentation) and

diagnosis (R^2 : 0.56 for T1 segmentation; R^2 : 0.78 for STIR segmentation) (Tables 3, 4).

10° Percentile and Autocorrelation showed a significant correlation with VA grading for T1 sequences analysis (Table 3); whereas Mean Absolute Deviation and run length non-uniformity showed significant correlation with VA for STIR sequences analysis (Table 4).

Regression model analysis identified one radiomic feature with significant correlation with VO (Gray Level non-uniformity Normalized, $p = 0.004$) and 6 radiomic features with significant correlation with diagnosis (High Gray Level Zone Emphasis, $p < 0.001$; Entropy, $p < 0.001$, for T1 segmentation; Mean Absolute Deviation, $p < 0.001$; Coarseness < 0.001 ; Small Area Low Gray Level Emphasis, $p < 0.001$; Contrast, $p = 0.008$, for STIR segmentation) (Tables 3, 4).

Significant differences were found between patients and control subjects for all radiomic features ($p < 0.05$) except for small dependence emphasis ($p = 0.128$), cluster shade ($p = 0.100$), difference entropy ($p = 0.152$), skewness ($p = 0.192$), run variance ($p = 0.173$), size zone non-uniformity normalized ($p = 0.280$), zone percentage ($p = 0.093$), small area emphasis ($p = 0.943$).

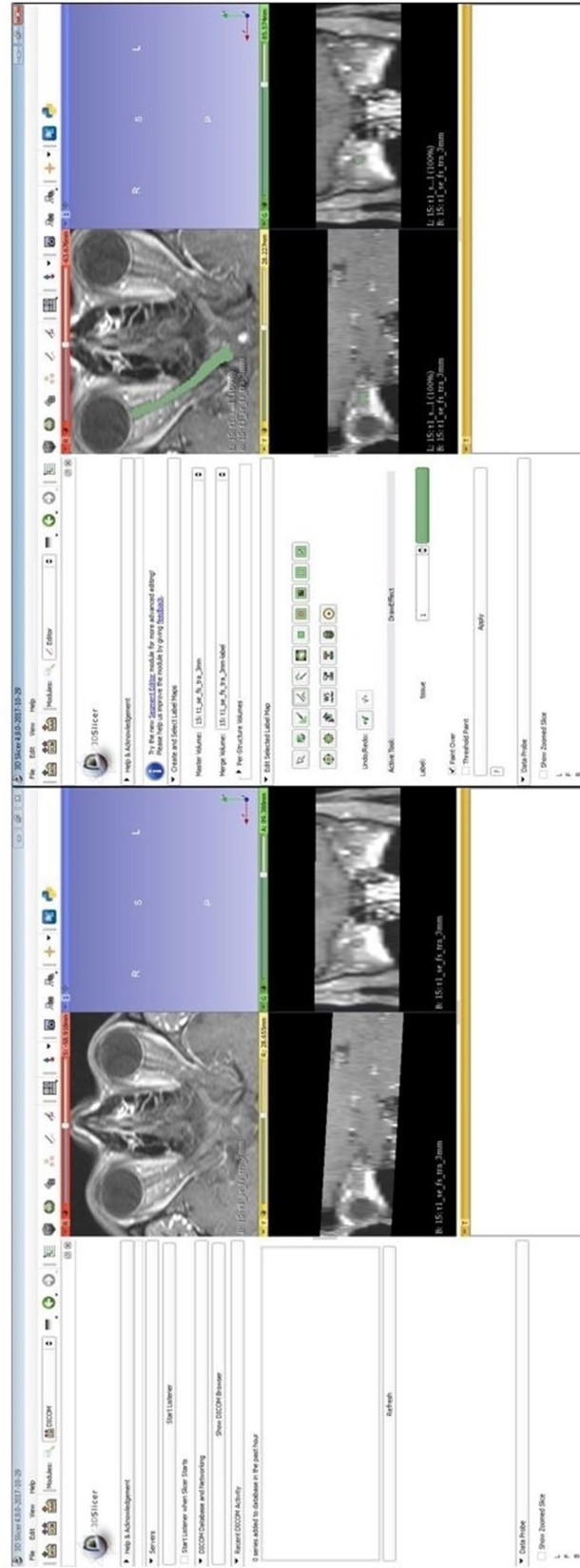


Fig. 2 Example of optic nerve segmentation on 3D slicer open-source software

Table 2 Results of the multivariate logistic regression analysis: correlations between radiomics variables and RNFL values of temporal (T) temporal superior (TS) nasal superior (NS) nasal (N) nasal inferior (NI) temporal inferior (TI) quadrants of the retina and global average RNFL value (G) at the OCT

		OR	Sig.	95% CI	
				Lower bound	Upper bound
Retinal quadrant	T				
Radiomics features	Skewness	.323	.009*	.000	.000
	90° percentile	.335	.045	.003	.232
	10° percentile	-.357	.063	-.423	.012
	Gray level variance	-.227	.010	.000	.000
	Interquartile range	.967	.000*	.541	.829
	Total energy	-.231	.048	.000	.000
	Gray level Non-Uniformity	.787	.000*	1.144	1.857
	Zone entropy	-.632	.000*	-53.791	-24.107
Retinal quadrant	TS				
Radiomics features	Median	-.239	.056	-.482	.007
	90° percentile	.426	.002*	.124	.506
	Gray level variance	-.204	.050	.000	.000
	Gray level Non-Uniformity	.466	.001*	.814	2.927
Retinal quadrant	NS				
Radiomics features	Energy	-.732	.011	.000	.000
	10° percentile	.323	.084	-.071	1.051
	Gray level Non-Uniformity	.909	.000*	2.537	6.597
	Zone Entropy	.315	.079	-6.309	108.549
Retinal quadrant	N				
Radiomics features	Energy	-.333	.085	.000	.000
	Median	.401	.014	.050	.393
	Gray level Non-Uniformity	.804	.000*	1.199	2.764
	High gray level zone emphasis	.385	.002*	.108	.429
Retinal quadrant	NI				
Radiomics features	Energy	.552	.002*	.000	.000
Retinal quadrant	TI				
Radiomics features	Median	.476	.014	.116	.935
	Energy	-.853	.001*	.000	.000
	Gray level variance	-.258	.058	.000	.000
	Gray level Non-Uniformity	.934	.000*	2.705	6.505
Global Average Value	G				
Radiomics features	Median	.459	.002*	.127	.518
	Energy	-.456	.041	.000	.000
	Gray level non-uniformity	1.107	.000*	2.483	4.457
	Flatness	-.429	.020	-735.252	-69.359
	Zone entropy	.260	.041	1.178	51.483

*Indicates the variables with *p* value < 0.01

Discussion

Acute inflammation of the optic nerve is often the first manifestation of MS, therefore, ON is considered as a model to investigate the relationship between structures and function [23] to forecast functional recovery of neurological deficit and establish long term MS treatments [24].

In this retrospective study, we demonstrated a correlation between radiomic features and RNFL thickness. The use of OCT revolutionized ophthalmology and

neuro-ophthalmologic practice and has become essential for the assessment of axonal integrity, evaluation of disease progression in the afferent visual pathway, and prediction of post-surgical VO in compressive optic neuropathies [23]. RNFL thickness has significant relationships with VA, visual field, color vision, VEPs amplitude, can be used as a biomarker of neurodegeneration in MS [25, 26], and to detect subclinical axonal loss in eyes with normal VA and visual field [23]. A strong correlation between RNFL thickness and VO has also been described [27, 28], hypothesizing that

Table 3 Results of regression analysis of radiomic features with visual acuity, visual outcome, and diagnosis for T1 segmentation

	Model	Coefficients		Standardized coefficients	<i>t</i>	<i>p</i>
		Beta	SE			
Visual acuity	Constant	2.693	0.509	5.293	5.293	0.000
	10° Percentile	−0.006	0.002	−0.468	−3.234	0.003*
	Autocorrelation	1.105E−12	0.000	0.439	3.034	0.005*
Visual outcome	Constant	1.169	0.394	2.966	2.966	0.006
	Gray level non-uniformity normalized	6.872	2.199	0.484	3.125	0.004*
	Total energy	−9.256E−13	0.000	−0.407	−2.632	0.014
Diagnosis	Constant	1.946	0.200	9.730	9.730	0.000
	High gray level zone emphasis	−1.120E−12	0.000	−0.651	−4.189	0.000*
	Entropy	−3.064E−12	0.000	−0.618	−4.102	0.000*
	Mean absolute deviation	9.766E−13	0.000	0.391	2.687	0.013
	Autocorrelation	7.128E−13	0.000	0.388	2.375	0.026

*Indicates the variables with *p* value < 0.01

Table 4 Results of regression analysis of radiomic features with visual acuity, visual outcome, and diagnosis for STIR segmentation

	Model	Coefficients		Standardized coefficients	<i>t</i>	<i>p</i>
		Beta	SE			
Visual acuity	Constant	3.631	0.409		8.876	< 0.001
	Mean absolute deviation	−1.669E−12	0.000	−0.770	−6.018	< 0.001*
	run length non-uniformity	−3.515E−12	0.000	−0.513	−3.988	0.001*
	Small dependence high gray level emphasis	7.257E−13	0.000	0.324	2.589	0.021
	Gray level variance	−1.047E−12	0.000	−0.296	−2.353	0.033
Visual outcome	Constant	0.418	0.640		0.653	0.522
	Difference average	7.601E−12	0.000	0.477	2.301	0.034
Diagnosis	Constant	−0.308	0.380		−0.811	0.431
	Mean absolute deviation	1.458E−12	0.000	0.919	8.001	< 0.001*
	coarseness	−102.145	13.075	−0.930	−7.812	< 0.001*
	Small area low gray level emphasis	121.811	15.247	1.029	7.989	< 0.001*
	Contrast	5.819	1.891	0.300	3.077	0.008*
	Sum entropy	1.171E−12	0.000	0.313	2.866	0.012

*Indicates the variables with *p* value < 0.01

a slower RNFL thinning in early ON is related to a better VO in MS [29]. Therefore, the correlation between radiomic features and RNFL thickness, suggests the promising role of radiomics as a tool in the study of demyelinating diseases.

We observed correlations between VA at presentation and radiomic features for both segmentation of T1 and STIR sequences: 10° Percentile, Autocorrelation, Mean Absolute Deviation, run length non-uniformity, and such data reinforce our hypothesis that radiomics could be considered a marker of pathological microstructural changes in optic nerves.

We also found correlations between VO at 6 months and Gray Level non-uniformity Normalized. Orbital MRI is considered the gold standard to grade optic nerve

inflammation through the evaluation of lesions length and enhancement activity [25], but its value in predicting the clinical outcome is still unclear, with studies describing no relationship between acute MRI optic nerve lesions and visual recovery [9, 10], and, on the other side, a study by Soelberg et al. who stated that optic nerve abnormalities extension was related to progressive degeneration [30]. Another study by Berg et al. reported that the length of optic nerve gadolinium enhancement and T2 hyperintensities in acute ON showed a medium correlation with VO [12]. Our results could represent a new perspective in predicting visual function recovery after the first episode of ON and an interesting starting point for future studies.

Zhang et al., in a study on 25 ON in relapsing–remitting MS or CIS [17], observed that heterogeneity at texture analysis was able to predict functional recovery. To the best of our knowledge, no other data regarding the relationships between radiomics and ON or its clinical outcome are available. However, the role of MRI texture analysis has been investigated in MS with promising results. Harrison et al., in a study on 38 MS patients, demonstrated that textural analysis provided an excellent distinction between MS plaques and normal-appearing white matter [31]. The texture analysis proved to be a measure of tissue integrity since texture heterogeneity was associated with worst myelin and axonal pathology, as demonstrated in postmortem MS brains from 3 subjects [32] and in vivo on 12 acute MS brain lesions [33]; these data can be explained by the fact that, when the myelin is disrupted, the tissue becomes disorganized and coarse texture increases. According to the severity of structural disorganization in acute MS lesion, MRI texture analysis can be used to predict persistent brain tissue damage [34] and to evaluate treatment impact [35].

As far as predicting patients' evolution in MS is concerned, we observed a significant correlation with high gray level zone emphasis and entropy for T1 segmentation and with Mean Absolute Deviation, Coarseness, Small Area Low Gray Emphasis, and Contrast for STIR analysis.

As the demyelination and axonal loss that take place in the optic nerves represent a model of alterations in white matter structures, ON can be applied as a paradigm for MS to establish the neuroprotective efficacy of novel therapeutics in clinical trials [13, 36, 37], therefore these preliminary results can be useful to support the application of radiomics in ON to identify patients with a worse clinical outcome who could benefit from new remyelinating therapeutic strategies, but also validate the use of radiomics in the wider group of MS patients.

This study has some limitations: firstly, the limited number of patients, then limiting broad conclusions and requiring confirmation on larger series, however, radiomics studies on small groups of patients have already been published, even recently [17, 33, 34, 38, 39], and, secondly, the radiomic analysis has been performed by only one operator.

Conclusions

Radiomic features correlate with visual functionality and VO in ON patients.

We confirmed that radiomic analysis has the potential to extract clinically meaningful information from conventional MRI and is a promising tool to predict visual recovery. It may become an attractive non-invasive tool for monitoring disease activity and assessing remyelination therapies in demyelinating processes.

Funding No funding has been received for this study.

Compliance with ethical standards

Conflict of interest The authors declare that they have no conflicts of interest.

Human or animals rights This retrospective study involving human participants has been approved by our Institutional Review Board.

Informed consent Informed written consent was provided by patients.

References

- Petzold A, Wattjes M, Costello F et al (2014) The investigation of acute optic neuritis: a review and proposed protocol. *Nat Rev Neurol* 10(8):447–458. <https://doi.org/10.1038/nrneurol.2014.108>
- Protti A, Spreafico C, Frigerio R et al (2004) Optic neuritis: diagnostic criteria application in clinical practice. *Neurol Sci* 25(Suppl 3):S296–S297
- Ghezzi A, Martinelli V, Rodegher M et al (2000) The prognosis of idiopathic optic neuritis. *Neurol Sci* 21(4 Suppl 2):S865–S869
- Huang-Link YM, Al-Hawasi A, Lindehammar H (2015) Acute optic neuritis: retinal ganglion cell loss precedes retinal nerve fiber thinning. *Neurol Sci* 36(4):617–620. <https://doi.org/10.1007/s10072-014-1982-3>
- Kolappan M, Henderson AP, Jenkins TM et al (2009) Assessing structure and function of the afferent visual pathway in multiple sclerosis and associated optic neuritis. *J Neurol* 256(3):305–319. <https://doi.org/10.1007/s00415-009-0123-z>
- Tas A, Altun S, Yolcu U et al (2015) Acute optic neuritis: retinal ganglion cell loss precedes retinal nerve fiber thinning. *Neurol Sci* 36(7):1277. <https://doi.org/10.1007/s10072-014-2011-2>
- Hirst CL, Ingram G, Pickersgill TP et al (2012) Temporal evolution of remission following multiple sclerosis relapse and predictors of outcome. *Mult Scler* 18(8):1152–1158. <https://doi.org/10.1177/1352458511433919>
- Cellina M, Floridi C, Rosti C et al (2019) MRI of acute optic neuritis (ON) at the first episode: can we predict the visual outcome and the development of multiple sclerosis (MS)? *Radiol Med.* <https://doi.org/10.1007/s11547-019-01073-1>
- Hickman SJ, Toosy AT, Miszkief KA et al (2004) Visual recovery following acute optic neuritis—a clinical, electrophysiological and magnetic resonance imaging study. *J Neurol* 251(8):996–1005. <https://doi.org/10.1007/s00415-004-0477-1>
- Kupersmith MJ, Mandel G et al (2011) Baseline, one and three month changes in the peripapillary retina nerve fiber layer in acute optic neuritis: relation to baseline vision and MRI. *J Neurol Sci* 308(1–2):117–123. <https://doi.org/10.1016/j.jns.2011.05.039>
- Jenkins TM, Toosy AT, Ciccarelli O (2010) Neuroplasticity predicts outcome of optic neuritis independent of tissue damage. *Ann Neurol* 67(1):99–113. <https://doi.org/10.1002/ana.21823>
- Berg S, Kaschka I, Utz KS et al (2015) Baseline magnetic resonance imaging of the optic nerve provides limited predictive information on short-term recovery after acute optic neuritis. *PLoS ONE* 10(1):e0113961. <https://doi.org/10.1371/journal.pone.0113961>
- McKee JB, Elston J, Evangelou N et al (2015) Amiloride clinical trial in optic neuritis (ACTION) protocol: a randomised, double

- blind, placebo controlled trial. *BMJ Open* 5(11):e009200. <https://doi.org/10.1136/bmjopen-2015-009200>
14. Gillies RJ, Kinahan PE, Hricak H (2016) Radiomics: images are more than pictures. *Data Radiol* 278(2):563–577. <https://doi.org/10.1148/radiol.2015151169>
 15. Zhang Y (2012) MRI texture analysis in multiple sclerosis. *Int J Biomed Imaging*. <https://doi.org/10.1155/2012/762804>
 16. Yip SS, Aerts HJ (2016) Applications and limitations of radiomics. *Phys Med Biol* 61(13):R150–66. <https://doi.org/10.1088/0031-9155/61/13/R150>
 17. Zhang Y, Metz LM, Scott JN et al (2014) MRI texture heterogeneity in the optic nerve predicts visual recovery after acute optic neuritis. *Neuroimage Clin* 14(4):302–307. <https://doi.org/10.1016/j.nicl.2014.01.003>
 18. Cellina M, Fetoni V, Ciocca M et al (2018) Anti-myelin oligodendrocyte glycoprotein antibodies: Magnetic resonance imaging findings in a case series and a literature review. *Neuroradiol J* 31(1):69–82. <https://doi.org/10.1177/1971400917698856>
 19. Fedorov A, Beiche R, Kalpathy Cramer J et al (2012) 3D Slicer as an Image Computing Platform for the Quantitative Imaging Network. *Magn Reson Imag* 30(9):1323–1341. <https://doi.org/10.1016/j.mri.2012.05.001>
 20. Pieper S, Halle M, Kikinis R (2004) 3D Slicer. *IEEE Int Symp Biomed Imag Nano Macro* 1:632–635
 21. Brusa A, Jones SJ, Plant GT (2001) Long-term remyelination after optic neuritis: A 2-year visual evoked potential and psychophysical serial study. *Brain* 124(Pt 3):468–479
 22. Thompson AJ, Banwell BL, Barkhof F et al (2018) Diagnosis of multiple sclerosis: 2017 revisions of the McDonald criteria. *Lancet Neurol* 17(2):162–173. [https://doi.org/10.1016/S1474-4422\(17\)30470-2](https://doi.org/10.1016/S1474-4422(17)30470-2)
 23. Jenkins T, Ciccarelli O, Toosy A et al (2010) Dissecting structure-function interactions in acute optic neuritis to investigate neuroplasticity. *Hum Brain Mapp* 31(2):276–286. <https://doi.org/10.1002/hbm.20863>
 24. Swanton JK, Fernando KT, Dalton CM et al (2010) Early MRI in optic neuritis: the risk for clinically definite multiple sclerosis. *Mult Scler* 16(2):156–165. <https://doi.org/10.1177/1352458509353650>
 25. Jankowska-Lech I, Wasyluk J, Palasik W et al (2018) Peripapillary retinal nerve fiber layer thickness measured by optical coherence tomography in different clinical subtypes of multiple sclerosis. *Mult Scler Relat Disord* 5(27):260–268. <https://doi.org/10.1016/j.msard.2018.11.003>
 26. Waldman AT, Hiremath G, Avery RA et al (2013) Monocular and binocular low-contrast visual acuity and optical coherence tomography in pediatric multiple sclerosis. *Mult Scler Relat Disord* 3(3):326–334. <https://doi.org/10.1016/j.msard.2013.10.008>
 27. Cettomai D, Hiremath G, Ratchford J et al (2010) Associations between retinal nerve fiber layer abnormalities and optic nerve examination. *Neurology* 75(15):1318–1325. <https://doi.org/10.1212/WNL.0b013e3181f735bd>
 28. Costello F, Coupland S, Hodge W et al (2006) Quantifying axonal loss after optic neuritis with optical coherence tomography. *Ann Neurol* 59(6):963–969. <https://doi.org/10.1002/ana.20851>
 29. Costello F, Burton JM (2018) Retinal imaging with optical coherence tomography: a biomarker in multiple sclerosis? *Eye Brain* 10:47–63. <https://doi.org/10.2147/EB.S139417>
 30. Soelberg K, Skejoe HPB, Grauslund J et al (2018) Magnetic resonance imaging findings at the first episode of acute optic neuritis. *Mult Scler Relat Disord* 20:30–36. <https://doi.org/10.1016/j.msard.2017.12.018>
 31. Harrison LC, Raunio M, Holli KK et al (2010) MRI texture analysis in multiple sclerosis: toward a clinical analysis protocol. *Acad Radiol* 17(6):696–707. <https://doi.org/10.1016/j.acra.2010.01.005>
 32. Zhang Y, Moore GR, Laul C et al (2013) Pathological correlates of magnetic resonance imaging texture heterogeneity in multiple sclerosis. *Ann Neurol* 74(1):91–99. <https://doi.org/10.1002/ana.23867>
 33. Zhang Y, Zhu H, Mitchell JR et al (2009) T2 MRI texture analysis is a sensitive measure of tissue injury and recovery resulting from acute inflammatory lesions in multiple sclerosis. *Neuroimage* 47(1):107–111. <https://doi.org/10.1016/j.neuroimage.2009.03.075>
 34. Zhang Y, Traboulsee A, Zhao Y et al (2011) Texture analysis differentiates persistent and transient T1 black holes at acute onset in multiple sclerosis: a preliminary study. *Mult Scler* 17(5):532–540. <https://doi.org/10.1177/1352458510395981>
 35. Cadavid D, Balcer L, Galetta S et al (2017) RENEW Study Investigators Safety and efficacy of opicinumab in acute optic neuritis (RENEW): a randomised, placebo-controlled, phase 2 trial. *Lancet Neurol* 16(3):189–199. [https://doi.org/10.1016/S1474-4422\(16\)30377-5](https://doi.org/10.1016/S1474-4422(16)30377-5)
 36. Takahashi H, Okuda S, Tamura M et al (2019) Prophylactic treatment with intravenous immunoglobulin attenuates experimental optic neuritis in mice. *Biol Pharm Bull* 42(2):173–178. <https://doi.org/10.1248/bpb.b18-00458>
 37. Tourbah A, Gout O, Vighetto A et al (2018) MD1003 (high-dose pharmaceutical-grade biotin) for the treatment of chronic visual loss related to optic neuritis in multiple sclerosis: a randomized, double-blind, Placebo-Controlled Study *CNS Drugs* 32(7):661–672. <https://doi.org/10.1007/s40263-018-0528-2>
 38. Zhang Y, Zhu Y, Shi X et al (2018) Soft tissue sarcomas: preoperative predictive histopathological grading based on radiomics of MRI. *Acad Radiol*. <https://doi.org/10.1016/j.acra.2018.09.025>
 39. Lecler A, Duron L, Balvay D et al (2019) Combining multiple magnetic resonance imaging sequences provides independent reproducible radiomics features. *Sci Rep* 9(1):2068. <https://doi.org/10.1038/s41598-018-37984-8>

Publisher's Note Springer Nature remains neutral with regard to jurisdictional claims in published maps and institutional affiliations.